Distributed Optimal Energy Management in Microgrids

Wenbo Shi, *Student Member, IEEE,* Xiaorong Xie, *Member, IEEE,* Chi-Cheng Chu, and Rajit Gadh

Abstract—Energy management in microgrids is typically formulated as a nonlinear optimization problem. Solving it in a centralized manner does not only require high computational capabilities at the microgrid central controller (MGCC), but may also infringe customer privacy. Existing distributed approaches, on the other hand, assume that all generations and loads are connected to one bus, and ignore the underlying power distribution network and the associated power flow and system operational constraints. Consequently, the schedules produced by those algorithms may violate those constraints and thus are not feasible in practice. Therefore, the focus of this paper is on the design of a distributed energy management strategy (EMS) for the optimal operation of microgrids with consideration of the distribution network and the associated constraints. Specifically, we formulate microgrid energy management as an optimal power flow problem, and propose a distributed EMS where the MGCC and the local controllers jointly compute an optimal schedule. We also provide an implementation of the proposed distributed EMS based on IEC 61850. As one demonstration, we apply the proposed distributed EMS to a real microgrid in Guangdong Province, China, consisting of photovoltaics, wind turbines, diesel generators, and a battery energy storage system. The simulation results demonstrate the effectiveness and fast convergence of the proposed distributed EMS.

Index Terms—Distributed algorithms, distribution networks, energy management, microgrids, optimal power flow (OPF), optimization.

I. INTRODUCTION

MICROGRIDS are low-voltage distribution systems consisting of distributed energy resources (DERs) and controllable loads, which can be operated in either islanded or grid-connected mode [2]. DERs include a variety of distributed generation (DG) units such as wind turbines (WTs), photovoltaics (PVs), and distributed storage (DS) units such as batteries. Sound operation of a microgrid requires an energy management strategy (EMS) which controls the power flows in the microgrid by adjusting the power imported/exported from/to the main grid, the dispatchable DERs, and the controllable loads based on the present and forecasted information of the market, the generations, and the loads in order to meet certain operational objectives (e.g., minimizing costs) [2].

Energy management in microgrids is typically formulated as a nonlinear optimization problem. Various centralized methods have been proposed to solve it in the literature, including mixed integer programming [3], sequential quadratic programming [4], particle swarm optimization [5], neural networks [6], etc. The centralized approaches [3]–[6] require high computational capabilities at the microgrid central controller (MGCC), which is neither efficient nor scalable. Moreover, a centralized EMS requires the MGCC to gather information of the DERs (e.g., production costs, constraints, etc.) and the loads (e.g., customer preferences, constraints, etc.) as the inputs for optimization. However, different DERs may belong to different entities and they may keep their information private [7]. Customers may also be unwilling to expose their information due to privacy [8]. Therefore, in this paper, we are interested in developing a distributed EMS which is efficient, scalable, and privacy preserving.

Several distributed algorithms have been proposed for the operation of microgrids in the literature. In [7], a distributed algorithm based on the classical symmetrical assignment problem is proposed. Energy management is formulated as a resource allocation problem in [9] and distributed algorithms are proposed for distributed allocation. A convex problem formulation can be found in [10] and dual decomposition is used to develop a distributed EMS to maintain the supply–demand balance in microgrids. A privacy-preserving energy scheduling algorithm in microgrids is proposed in [8], where the privacy constraints are integrated with the linear programming model and distributed algorithms are developed. In [11], the additive-increase/multiplicative-decrease algorithm is adopted to optimize DER operations in a distributed fashion.

The problem with the existing distributed approaches for microgrid energy management [7]–[11] is that they consider the supply–demand matching in an abstract way where the aggregate demand is simply equal to the supply. They assume that all generations and loads are connected to one bus and ignore the underlying power distribution network and the associated power flow (e.g., Kirchhoff's law) and system operational constraints (e.g., voltage tolerances). Consequently, the schedules produced by those algorithms may violate those constraints and thus are not feasible in practice. It is worth noting that distribution networks have been taken into account

W. Shi, C.-C. Chu, and R. Gadh are with the Smart Grid Energy Research Center, University of California, Los Angeles, CA 90095 USA (e-mail: wenbos@ucla.edu).

X. Xie is with the State Key Laboratory of Power Systems, Department of Electrical Engineering, Tsinghua University, Beijing 100084, China.

in a few recent demand response studies [12]. However, the idea of integrating distribution networks with distributed energy management in microgrids, where both supply-side and demand-side management (DSM) are considered has not been explored.

The focus of this paper is on the design of a distributed EMS for the optimal operation of microgrids with consideration of the underlying power distribution network and the associated constraints. More specifically, we consider a microgrid consisting of multiple DERs and controllable loads. The objective of the EMS is to control the power flows in the microgrid in order to: 1) minimize the cost of generation, the cost of energy storage, and the cost of energy purchase from the main grid; 2) minimize the dissatisfactions of the customers in the DSM; and 3) minimize the power losses subject to the DER constraints, the load constraints, the power-flow constraints, and the system operational constraints.

Specifically, we formulate energy management in microgrids as an optimal power flow (OPF) problem. The OPF problem is difficult to solve due to the nonconvex power-flow constraints. We convexify the OPF problem by relaxing the power-flow constraints (see [13], [14] for a tutorial on convex relaxation of OPF). Sufficient conditions for the exactness of the relaxation have been derived in [15]–[18], which hold for a variety of IEEE test systems and real-world systems. Therefore, we focus on solving the relaxed OPF problem (OPF-r) in this paper. Note that most of the convex relaxations of OPF [15]–[18] assume a single-phase or balanced three-phase distribution network. See [19] for convex relaxation of OPF in multiphase networks. The OPF-r problem is a centralized convex optimization problem. To solve it in a distributed manner, we propose a distributed EMS where the MGCC and the local controllers (LCs) jointly compute an optimal schedule.

In order to illustrate the feasibility of the proposed EMS in real systems, we provide an implementation based on the IEC 61850 standard which provides standardized communication and control interfaces for all DER devices. As one demonstration, we apply the proposed EMS to a real microgrid in Guangdong Province, China, consisting of PVs, WTs, diesel generators, and a battery energy storage system (BESS). The simulation results demonstrate the effectiveness and fast convergence of the proposed EMS. We show that the proposed EMS is able to manage the operations in the microgrid to achieve the objective while maintaining the bus voltages within the allowed range. Furthermore, we discuss the location effect, the load shedding/shifting, the ramping constraint, and the trade-offs in the objective.

Compared with a preliminary version of this paper [1], this paper provides a more realistic and detailed system model by incorporating the generation ramping constraint, the inverter capacity, the battery efficiency, and the load shifting. We also provide an IEC 61850 implementation of the proposed distributed EMS to demonstrate its feasibility in real systems. A case study using the real pricing data is provided to give better insights into microgrid energy management. A more comprehensive analysis of the proposed EMS is given, including the discussions on the location effect, the load
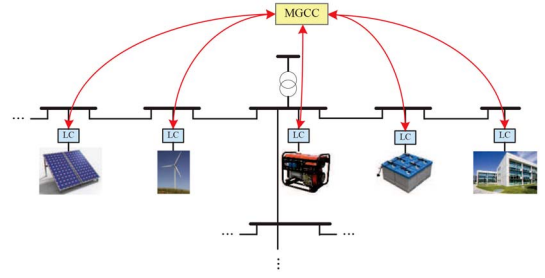

Fig. 1. System architecture.

shedding/shifting, the ramping constraint, and the trade-offs in the objective.

The rest of this paper is organized as follows. We introduce the system model in Section II and propose the EMS in Section III. Simulation results are provided in Section V and the conclusion is given in Section VI.

II. SYSTEM MODEL

In this section, we describe the system model for developing the proposed distributed EMS. We first give an overview of the system followed by the DG model, the DS model, and the load model. We then model the power distribution network using a branch flow model and formulate microgrid energy management as an OPF problem.

A. System Overview

A low-voltage power distribution network generally has a radial structure [12]. Thus, we consider a radial microgrid consisting of a set of DG units denoted by $\mathcal{G} \triangleq \{g_1, g_2, \ldots, g_G\}$, DS units denoted by $\mathcal{B} \triangleq \{b_1, b_2, \ldots, b_B\}$, and controllable loads denoted by $\mathcal{L} \triangleq \{l_1, l_2, \ldots, l_L\}$. In the microgrid, there is a MGCC which coordinates the operations of the DERs and the controllable loads. At each of the DERs and the loads, there is a LC which is able to coordinate with the MGCC to compute its schedule locally via a two-way communication infrastructure. Fig. 1 shows the system architecture.

In this paper, we use a discrete-time model with a finite horizon. We consider a time period or namely a scheduling horizon, which is divided into T equal intervals Δt, denoted by $\mathcal{T} \triangleq \{0, 1, \ldots, T - 1\}$.

B. DG Model

We consider both renewable and conventional DGs in the microgrid. Renewable DGs such as PVs and WTs are nondispatchable and conventional DGs such as diesel are dispatchable. For each DG $g \in \mathcal{G}$, we denote its complex output power by $s_g(t) \triangleq p_g(t) + \mathbf{i}q_g(t)$, where $p_g(t)$ is the active power and $q_g(t)$ is the reactive power.

1) Renewable DG: A renewable DG unit such as PV or WT is not dispatchable and its output power is dependent on the availability of the primary sources (i.e., sun irradiance or wind). Therefore, forecast is required in order to consider them in the energy management optimization. Methods for PV forecasting [20] and WT forecasting [21] can be utilized. In

our model, we assume that the complex power of a renewable DG unit over the scheduling horizon is given and there is no generation cost for renewable DGs.

2) Conventional DG: A conventional DG unit such as diesel is a dispatchable source, its output power is a variable with the following constraints:

$$0 \leq p_g(t) \leq \bar{p}_g, \qquad \forall t \in \mathcal{T}, \tag{1}$$

$$|p_g(t) - p_g(t-1)| \leq r_g \bar{p}_g, \quad \forall t \in \mathcal{T}, \tag{2}$$

where $\bar{p}_g$ is the maximum output power and $r_g \in (0, 1]$ is the ramping parameter.

For a given conventional DG unit, its reactive power generated at the inverter is bounded by

$$p_g(t)^2 + q_g(t)^2 \leq s_g^2, \ \forall t \in \mathcal{T}, \tag{3}$$

where s_g is the capacity of the inverter.

We model the conventional DG generation cost at each time $t \in \mathcal{T}$ using a quadratic model [10]

$$C_g(p_g(t)) \triangleq \alpha_g \left(p_g(t)\Delta t\right)^2 + \beta_g p_g(t)\Delta t + c_g, \tag{4}$$

where α_g, β_g, and c_g are constants.

C. DS Model

We consider batteries as the DS units in the microgrid. For a given battery $b \in \mathcal{B}$, we denote its complex power by $s_b(t) \triangleq p_b(t) + \mathbf{i}q_b(t)$, where $p_b(t)$ is the active power (positive when charging and negative when discharging) and $q_b(t)$ is the reactive power. Let $E_b(t)$ denote the energy stored in the battery at time t. A given battery can be modeled by the following constraints:

$$\underline{p}_b \leq p_b(t) \leq \bar{p}_b, \ \forall t \in \mathcal{T}, \tag{5}$$

$$p_b(t)^2 + q_b(t)^2 \leq s_b^2, \ \forall t \in \mathcal{T}, \tag{6}$$

$$E_b(t+1) = \eta_b E_b(t) + p_b(t)\Delta t, \ \forall t \in \mathcal{T}, \tag{7}$$

$$\underline{E}_b \leq E_b(t) \leq \bar{E}_b, \ \forall t \in \mathcal{T}, \tag{8}$$

$$E_b(T) \geq E_b^e, \tag{9}$$

where $\bar{p}_b$ is the maximum charging rate, $-\underline{p}_b$ is the maximum discharging rate, s_b is the capacity of the inverter, $\eta_b \in (0, 1]$ captures the battery efficiency, $\underline{E}_b$ and $\bar{E}_b$ are the minimum and maximum allowed energy stored in the battery, respectively, and E_b^e is the minimum energy that the battery should maintain at the end of the scheduling horizon.

We use a cost function to capture the damages to the battery by the charging and discharging operations. Three types of damages are considered: 1) fast charging; 2) frequent switches between charging and discharging; and 3) deep discharging. We model the battery cost as [22]

$$C_b(\mathbf{p}_b) \triangleq \alpha_b \sum_{t \in \mathcal{T}} p_b(t)^2 - \beta_b \sum_{t=0}^{T-2} p_b(t+1)p_b(t)$$
$$+ \gamma_b \sum_{t \in \mathcal{T}} \left(\min(E_b(t) - \delta_b \bar{E}_b, 0)\right)^2, \tag{10}$$

where $\mathbf{p}_b \triangleq (p_b(t), t \in \mathcal{T})$ is the charging/discharging vector, α_b, β_b, γ_b, and δ_b are positive constants. α_b, β_b, and γ_b

trade off among fast charging, switches between charging and discharging, and deep discharging. The above function is convex when $\alpha_b > \beta_b$. We choose $\delta_b = 0.2$, meaning that the cost function penalizes deep charging when the energy stored in the battery $E_b(t)$ is less than 20% of the battery capacity $\bar{E}_b$.

D. Load Model

We consider two types of controllable loads in the microgrid: interruptible and deferrable loads. An interruptible load can be shedded and a deferrable load can be shifted in time but need to consume a certain amount of energy before a deadline.

For each load $l \in \mathcal{L}$, we denote its complex power by $s_l(t) \triangleq p_l(t) + \mathbf{i}q_l(t)$ and it is bounded by

$$\underline{p}_l(t) \leq p_l(t) \leq \bar{p}_l(t), \ \forall t \in \mathcal{T}, \tag{11}$$

$$\underline{q}_l(t) \leq q_l(t) \leq \bar{q}_l(t), \ \forall t \in \mathcal{T}, \tag{12}$$

where $\underline{p}_l(t)$ and $\bar{p}_l(t)$ are the minimum and maximum active power, respectively, and $\underline{q}_l(t)$ and $\bar{q}_l(t)$ are the minimum and maximum reactive power, respectively.

For a deferrable load, we assume that its consumed energy is bounded by

$$\underline{E}_l \leq \sum_{t \in \mathcal{T}} p_l(t)\Delta t \leq \bar{E}_l, \tag{13}$$

where $\underline{E}_l$ and $\bar{E}_l$ are the energy lower and upper bound, respectively.

For each load, we define a demand vector denoted by $\mathbf{p}_l \triangleq (p_l(t), t \in \mathcal{T})$ and a cost function $C_l(\mathbf{p}_l)$ which measures the dissatisfaction of the customer using the demand schedule $\mathbf{p}_l$.

The cost function of an interruptible load is dependent on the shedded load and can be defined as

$$C_l(\mathbf{p}_l) \triangleq \sum_{t \in \mathcal{T}} \alpha_l \left(\min\left(p_l(t) - p_l^f(t), 0\right)\right)^2, \tag{14}$$

where $p_l^f(t)$ is the forecasted load and α_l is a positive constant. The above cost function is nonzero only when there is load shedding, i.e., $p_l(t) < p_l^f(t)$.

The cost function of a deferrable load is dependent on the unfulfilled energy and can be defined as

$$C_l(\mathbf{p}_l) \triangleq \alpha_l \left(\bar{E}_l - \sum_{t \in \mathcal{T}} p_l(t)\Delta t\right), \tag{15}$$

where α_l is a positive constant.

E. Distribution Network Model

A distribution network can be modeled as a connected graph $\mathcal{G} = (\mathcal{N}, \mathcal{E})$, where each node $i \in \mathcal{N}$ represents a bus and each link in $\mathcal{E}$ represents a branch (line or transformer). We denote a link by $(i, j) \in \mathcal{E}$. Power distribution networks are typically radial and the graph $\mathcal{G}$ becomes a tree for radial distribution systems. We index the buses in $\mathcal{N}$ by $i = 0, 1, \ldots, n$, and bus 0 denotes the feeder which has a fixed voltage and flexible power injection.

For each link $(i, j) \in \mathcal{E}$, let $z_{ij} \triangleq r_{ij} + \mathbf{i}x_{i,j}$ be the complex impedance of the branch, $I_{ij}(t)$ be complex current from buses i to j, and $S_{ij}(t) \triangleq P_{ij}(t) + \mathbf{i}Q_{ij}(t)$ be the complex power flowing from buses i to j.

For each bus $i \in \mathcal{N}$, let $V_i(t)$ be the complex voltage at bus i and $s_i(t) \triangleq p_i(t) + \mathbf{i}q_i(t)$ be the net load which is the load minus the generation at bus i. Each bus $i \in \mathcal{N} \setminus \{0\}$ is connected to a subset of DG units $\mathcal{G}_i$, DS units $\mathcal{B}_i$, and loads $\mathcal{L}_i$. The net load at each bus i satisfies

$$s_i(t) = s_{li}(t) + s_{bi}(t) - s_{gi}(t), \quad \forall i \in \mathcal{N} \setminus \{0\}, \forall t \in \mathcal{T}, \quad (16)$$

where $s_{li}(t) \triangleq \sum_{l \in \mathcal{L}_i} s_l(t)$, $s_{bi}(t) \triangleq \sum_{b \in \mathcal{B}_i} s_b(t)$, and $s_{gi} \triangleq \sum_{g \in \mathcal{G}_i} s_g(t)$.

Given the radial distribution network $\mathcal{G}$, the feeder voltage V_0, and the impedances $\{z_{ij}\}_{(i,j) \in \mathcal{E}}$, then the other variables including the power flows, the voltages, the currents, and the bus loads satisfy the following physical laws for all branches $(i, j) \in \mathcal{E}$ and all $t \in \mathcal{T}$.

1) Ohm's law:

$$V_i(t) - V_j(t) = z_{ij}I_{ij}(t). \quad (17)$$

2) Power-flow definition:

$$S_{ij}(t) = V_i(t)I_{ij}^*(t). \quad (18)$$

3) Power balance:

$$S_{ij}(t) - z_{ij}|I_{ij}(t)|^2 - \sum_{k:(j,k) \in \mathcal{E}} S_{jk}(t) = s_j(t). \quad (19)$$

Using (17)–(19) and in terms of real variables, we can model the steady-state power flows in a given distribution network $\mathcal{G}$ as [13]: $\forall (i, j) \in \mathcal{E}, \forall t \in \mathcal{T}$

$$p_j(t) = P_{ij}(t) - r_{ij}\ell_{ij}(t) - \sum_{k:(j,k) \in \mathcal{E}} P_{jk}(t), \quad (20)$$

$$q_j(t) = Q_{ij}(t) - x_{ij}\ell_{ij}(t) - \sum_{k:(j,k) \in \mathcal{E}} Q_{jk}(t), \quad (21)$$

$$v_j(t) = v_i(t) - 2\left(r_{ij}P_{ij}(t) + x_{ij}Q_{ij}(t)\right) + \left(r_{ij}^2 + x_{ij}^2\right)\ell_{ij}(t), \quad (22)$$

$$\ell_{ij}(t) = \frac{P_{ij}(t)^2 + Q_{ij}(t)^2}{v_i(t)}, \quad (23)$$

where $\ell_{ij}(t) \triangleq |I_{ij}(t)|^2$ and $v_i(t) \triangleq |V_i(t)|^2$.

Equations (20)–(23) define a system of equations in the variables $(\mathbf{P}(t), \mathbf{Q}(t), \mathbf{v}(t), \mathbf{l}(t), \mathbf{s}(t))$, where $\mathbf{P}(t) \triangleq (P_{ij}(t), (i, j) \in \mathcal{E})$, $\mathbf{Q}(t) \triangleq (Q_{ij}(t), (i, j) \in \mathcal{E})$, $\mathbf{v}(t) \triangleq (v_i(t), i \in \mathcal{N} \setminus \{0\})$, $\mathbf{l}(t) \triangleq (\ell_{ij}(t), (i, j) \in \mathcal{E})$, and $\mathbf{s}(t) \triangleq (s_i(t), i \in \mathcal{N} \setminus \{0\})$. The phase angles of the voltages and the currents are not included. But they can be uniquely determined for radial systems [14].

F. Energy Management

The objective of the microgrid operator is to minimize its operational cost, while delivering reliable and high-quality power to the loads. However, the introduction of DERs makes it challenging to balance the supply and demand in a microgrid, especially in islanded mode where only DERs are used as the supply. The integration of DERs may also increase the

voltage significantly, which reduces the quality of the voltage received by other users in the distribution network. Thus, in this paper, we study microgrid energy management aiming at achieving the operational objective of the microgrid operator, while meeting the supply–demand balance and the voltage tolerance constraints.

We consider the following voltage tolerance constraints in the microgrid:

$$\underline{V}_i \leq |V_i(t)| \leq \bar{V}_i, \quad \forall i \in \mathcal{N} \setminus \{0\}, \forall t \in \mathcal{T}, \quad (24)$$

where $\underline{V}_i$ and $\bar{V}_i$ correspond to the minimum and maximum allowed voltage according to the specification, respectively.

The net power injected to the microgrid from the main grid is given by

$$s_0(t) = \sum_{j:(0,j) \in \mathcal{E}} s_{0j}(t), \quad \forall t \in \mathcal{T}. \quad (25)$$

If the microgrid is operated in islanded mode, then $s_0(t) = 0$. If the microgrid is operated in grid-connected mode, then $s_0(t)$ is the net complex power traded between the microgrid and the main grid.

We model the cost of energy purchase from the main grid at each time $t \in \mathcal{T}$ as

$$C_0(t, p_0(t)) \triangleq \rho(t)p_0(t)\Delta t, \quad (26)$$

where $\rho(t)$ is the market energy price. Note that $p_0(t)$ can be negative, meaning that the microgrid can sell its surplus power to the main grid.

The objective of the energy management in the microgrid is to: 1) minimize the cost of generation, the cost of energy storage, and the cost of energy purchase from the main grid; 2) minimize the dissatisfactions of the customers in the DSM; and 3) minimize the power losses subject to the DER constraints, the load constraints, the power-flow constraints, and the system operational constraints (voltage tolerances).

We define $\mathbf{P} \triangleq (\mathbf{P}(t), t \in \mathcal{T})$, $\mathbf{Q} \triangleq (\mathbf{Q}(t), t \in \mathcal{T})$, $\mathbf{v} \triangleq (\mathbf{v}(t), t \in \mathcal{T})$, $\mathbf{l} \triangleq (\mathbf{l}(t), t \in \mathcal{T})$, $\mathbf{s}_g \triangleq (s_g(t), t \in \mathcal{T})$, $\mathbf{s}_b \triangleq (s_b(t), t \in \mathcal{T})$, $\mathbf{s}_l \triangleq (s_l(t), t \in \mathcal{T})$, $\mathbf{s} \triangleq (\mathbf{s}_g, \mathbf{s}_b, \mathbf{s}_l, g \in \mathcal{G}, b \in \mathcal{B}, l \in \mathcal{L})$, and $C_g(\mathbf{p}_g) \triangleq \sum_{t \in \mathcal{T}} C_g(p_g(t))$. Microgrid energy management can be formulated as an OPF problem

OPF

$$\min_{\mathbf{P}, \mathbf{Q}, \mathbf{v}, \mathbf{l}, \mathbf{s}} \quad \xi_g \sum_{g \in \mathcal{G}} C_g(\mathbf{p}_g) + \xi_b \sum_{b \in \mathcal{B}} C_b(\mathbf{p}_b) + \xi_l \sum_{l \in \mathcal{L}} C_l(\mathbf{p}_l)$$

$$+ \xi_0 \sum_{t \in \mathcal{T}} C_0(t, p_0(t)) + \xi_p \sum_{t \in \mathcal{T}} \sum_{(i,j) \in \mathcal{E}} r_{ij}\ell_{ij}(t)$$

$$\text{s.t.} \quad (1)\text{–}(3), (5)\text{–}(9), (11)\text{–}(13), (16),$$

$$(20)\text{–}(25),$$

where ξ_g, ξ_b, ξ_l, ξ_0, and ξ_p are the parameters to trade off among the cost minimizations and the power loss minimization.

III. DISTRIBUTED EMS

The previous OPF problem is nonconvex due to the quadratic equality constraint in (23) and is NP-hard to solve

in general [13]. We, therefore, relax them to inequalities

$$\ell_{ij}(t) \geq \frac{P_{ij}(t)^2 + Q_{ij}(t)^2}{v_i(t)}, \quad \forall (i,j) \in \mathcal{E}, \forall t \in \mathcal{T}. \quad (27)$$

We then consider the following convex relaxation of OPF:

OPF − r

$$\min_{\mathbf{P},\mathbf{Q},\mathbf{v},\mathbf{l},\mathbf{s}} \quad \xi_g \sum_{g \in \mathcal{G}} C_g(\mathbf{p}_g) + \xi_b \sum_{b \in \mathcal{B}} C_b(\mathbf{p}_b) + \xi_l \sum_{l \in \mathcal{L}} C_l(\mathbf{p}_l)$$

$$+ \xi_0 \sum_{t \in \mathcal{T}} C_0(t, p_0(t)) + \xi_p \sum_{t \in \mathcal{T}} \sum_{(i,j) \in \mathcal{E}} r_{ij} \ell_{ij}(t)$$

$$\text{s.t.} \quad (1)–(3), (5)–(9), (11)–(13), (16),$$
$$(20)–(22), (24), (25), (27).$$

If the equality in (27) is attained in the solution to OPF-r, then it is also an optimal solution to OPF. The sufficient conditions under which the relaxation is exact have been exploited in [15]–[18]. Roughly speaking, if the bus voltage is kept around the nominal value and the power injection at each bus is not too large, then the relaxation is exact. Detailed conditions when the voltage upper bound is not important can be found in [15] and [16]. See [17], [18] on how to deal with the voltage upper bound. In this paper, we assume that the sufficient conditions specified in [18] hold for the microgrid and thus we focus on solving the OPF-r problem.

The above OPF-r problem is a centralized optimization problem. In order to design an efficient, scalable, and privacy-preserving EMS, we propose a distributed algorithm to solve the OPF-r problem using the predictor corrector proximal multiplier (PCPM) algorithm (refer to [23] or the Appendix for details). Note that we use PCPM to develop the proposed distributed algorithm here. Other distributed algorithms such as the alternating direction method of multipliers (ADMM) algorithm [24] may also apply to solve the OPF-r problem in a distributed manner.

Initially set $k \leftarrow 0$. The LCs of the DERs and the loads set their initial schedules randomly and communicate them to the MGCC. In the meantime, the MGCC randomly chooses the initial $s_i^k(t) \triangleq p_i^k(t) + \mathbf{i} q_i^k(t)$ and two virtual control signals $\{\mu_i^k(t)\}_{t \in \mathcal{T}}$, $\{\lambda_i^k(t)\}_{t \in \mathcal{T}}$ for each bus $i \in \mathcal{N} \setminus \{0\}$. $\mu_i(t)$ and $\lambda_i(t)$ are the Lagrangian multipliers associated with the active and reactive power at bus i, respectively.

At the beginning of the kth step, the MGCC sends two control signals $\hat{\mu}_i^k(t) \triangleq \mu_i^k(t) + \gamma (p_{li}^k(t) + p_{bi}^k(t) - p_{gi}^k(t) - p_i^k(t))$ and $\hat{\lambda}_i^k(t) \triangleq \lambda_i^k(t) + \gamma (q_{li}^k(t) + q_{bi}^k(t) - q_{gi}^k(t) - q_i^k(t))$ to the LCs of the DERs and the loads connected to bus i, where γ is a positive constant. Then the following occurs.

1) The LC of each conventional DG unit solves the following problem:

EMS − LC(DG)

$$\min_{\mathbf{s}_g} \quad \xi_g C_g(\mathbf{p}_g) + \left(\hat{\boldsymbol{\mu}}_i^k\right)^T \mathbf{p}_g + \left(\hat{\boldsymbol{\lambda}}_i^k\right)^T \mathbf{q}_g$$

$$+ \frac{1}{2\gamma} \left\| \mathbf{p}_g - \mathbf{p}_g^k \right\|^2 + \frac{1}{2\gamma} \left\| \mathbf{q}_g - \mathbf{q}_g^k \right\|^2$$

$$\text{s.t.} \quad (1) - (3),$$

where $\hat{\boldsymbol{\mu}}_i^k \triangleq (\hat{\mu}_i^k(t), t \in \mathcal{T})$ and $\hat{\boldsymbol{\lambda}}_i^k \triangleq (\hat{\lambda}_i^k(t), t \in \mathcal{T})$. The optimal $\mathbf{s}_g^*$ is set as $\mathbf{s}_g^{k+1}$.

Algorithm 1 Proposed Distributed EMS

1: **initialization** $k \leftarrow 0$. The LCs set the initial schedules randomly and return them to the MGCC. The MGCC sets the initial $\mu_i^k(t)$, $\lambda_i^k(t)$ and the initial $s_i^k(t)$ randomly.
2: **repeat**
3:     The MGCC updates $\hat{\mu}_i^k(t)$ and $\hat{\lambda}_i^k(t)$ and sends two control signals $\hat{\boldsymbol{\mu}}_i^k$ and $\hat{\boldsymbol{\lambda}}_i^k$ to the LCs connected to bus i.
4:     The LC at each DER and each load calculates a new schedule by solving the corresponding EMS-LC problem.
5:     The MGCC computes a new $\mathbf{s}^{k+1}(t)$ for each time $t \in \mathcal{T}$ by solving the EMS-MGCC problem.
6:     The LC communicates the new schedule to the MGCC.
7:     The MGCC updates $\mu_i^{k+1}(t)$ and $\lambda_i^{k+1}(t)$.
8:     $k \leftarrow k + 1$.
9: **until** convergence

2) The LC of each DS unit solves the following problem:

EMS − LC(DS)

$$\min_{\mathbf{s}_b} \quad \xi_b C_b(\mathbf{p}_b) + \left(\hat{\boldsymbol{\mu}}_i^k\right)^T \mathbf{p}_b + \left(\hat{\boldsymbol{\lambda}}_i^k\right)^T \mathbf{q}_b$$

$$+ \frac{1}{2\gamma} \left\| \mathbf{p}_b - \mathbf{p}_b^k \right\|^2 + \frac{1}{2\gamma} \left\| \mathbf{q}_b - \mathbf{q}_b^k \right\|^2$$

$$\text{s.t.} \quad (5) - (9).$$

The optimal $\mathbf{s}_b^*$ is set as $\mathbf{s}_b^{k+1}$.

3) The LC of each load solves the following problem:

EMS − LC(Load)

$$\min_{\mathbf{s}_l} \quad \xi_l C_l(\mathbf{p}_l) + \left(\hat{\boldsymbol{\mu}}_i^k\right)^T \mathbf{p}_l + \left(\hat{\boldsymbol{\lambda}}_i^k\right)^T \mathbf{q}_l$$

$$+ \frac{1}{2\gamma} \left\| \mathbf{p}_l - \mathbf{p}_l^k \right\|^2 + \frac{1}{2\gamma} \left\| \mathbf{q}_l - \mathbf{q}_l^k \right\|^2$$

$$\text{s.t.} \quad (11)–(13).$$

The optimal $\mathbf{s}_l^*$ is set as $\mathbf{s}_l^{k+1}$.

4) The MGCC solves the following problem for each time $t \in \mathcal{T}$:

EMS − MGCC

$$\min_{\substack{\mathbf{P}(t),\mathbf{Q}(t), \\ \mathbf{v}(t),\mathbf{l}(t),\mathbf{s}(t)}} \quad \xi_0 C_0(t, p_0(t)) + \xi_p \sum_{(i,j) \in \mathcal{E}} r_{ij} \ell_{ij}(t)$$

$$- \left(\hat{\boldsymbol{\mu}}^k(t)\right)^T \mathbf{p}(t) - \left(\hat{\boldsymbol{\lambda}}^k(t)\right)^T \mathbf{q}(t)$$

$$+ \frac{1}{2\gamma} \left\| \mathbf{p}(t) - \mathbf{p}^k(t) \right\|^2 + \frac{1}{2\gamma} \left\| \mathbf{q}(t) - \mathbf{q}^k(t) \right\|^2$$

$$\text{s.t.} \quad (20)–(22), (24), (25), (27),$$

where $\hat{\boldsymbol{\mu}}^k(t) \triangleq (\hat{\mu}_i^k(t), i \in \mathcal{N} \setminus \{0\})$ and $\hat{\boldsymbol{\lambda}}^k(t) \triangleq (\hat{\lambda}_i^k(t), i \in \mathcal{N} \setminus \{0\})$. The optimal $\mathbf{s}^*(t)$ is set as $\mathbf{s}^{k+1}(t)$.

At the end of the kth step, the LCs communicate their new schedules $\mathbf{s}_l^{k+1}$, $\mathbf{s}_g^{k+1}$, and $\mathbf{s}_b^{k+1}$ to the MGCC and the MGCC updates $\mu_i^{k+1}(t) \triangleq \mu_i^k(t) + \gamma (p_{li}^{k+1}(t) + p_{bi}^{k+1}(t) - p_{gi}^{k+1}(t) - p_i^{k+1}(t))$ and $\lambda_i^{k+1}(t) \triangleq \lambda_i^k(t) + \gamma (q_{li}^{k+1}(t) + q_{bi}^{k+1}(t) - q_{gi}^{k+1}(t) - q_i^{k+1}(t))$ for all $i \in \mathcal{N} \setminus \{0\}$ and all $t \in \mathcal{T}$. Set $k \leftarrow k + 1$, and repeat the process until convergence.

A complete description of the proposed distributed EMS can be found in Algorithm 1. When γ is small enough, the above algorithm will converge to the optimal solution to OPF-r which
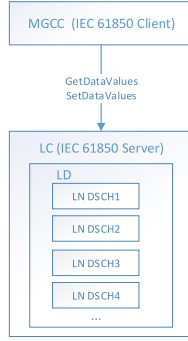
Fig. 2.   IEC 61850 implementation.

Fig. 3.   Topology of the microgrid.

is also the optimal solution to OPF if the relaxation is exact and $(p_{li}^k(t)+p_{bi}^k(t)-p_{gi}^k(t)-p_i^k(t))$ and $(q_{li}^k(t)+q_{bi}^k(t)-q_{gi}^k(t)-q_i^k(t))$ will converge to zero [23]. As we can see, the MGCC and the LCs jointly compute the optimal schedule.

In the proposed distributed EMS, the private information of the DERs and the loads is stored at the LC where the EMS-LC problem is solved locally. The MGCC solves the EMS-MGCC problem using the system information, including the topology, the power losses, the market energy price, etc. The information exchanged between the MGCC and the LCs include only the control signals and the schedules. Therefore, the privacy of the DERs (i.e., production costs and constraints) and the loads (i.e., customer preferences and constraints) are both preserved by the proposed EMS.

IV. IEC 61850 IMPLEMENTATION

IEC 61850 is a set of international standards designed originally for communications within substation automation systems [25]. More recently, IEC 61850 draws attention to researchers in the area of microgrids as it provides standardized communication and control interfaces for all DER devices to achieve interoperability in microgrids. Due to its essential role in microgrid systems, it is important that the microgrid EMS is compatible with IEC 61850. To this end, we provide an implementation of the proposed distributed EMS based on the IEC 61850 standard.

In IEC 61850, each DER unit is modeled as a logical device (LD). The LD is composed of the relevant logical nodes (LNs) which are predefined groupings of data objects that serve specific functions. Refer to [26] for detailed definitions of LNs for DER devices. The LN named DER energy and ancillary services schedule (DSCH) can be used to implement the proposed EMS. In a DSCH LN, an array of the timestamps and values can be read or written using the IEC 61850 ACSI services (e.g., GetDataValues and SetDataValues) and multiple schedules can be defined in parallel.

In order to implement the proposed EMS, we use four DSCH LNs: active power, reactive power, price for active power, and price for reactive power. The active power and reactive schedules are the results from solving the EMS-LC problem. The control signals sent by the MGCC $\hat{\mu}_i^k$ and $\hat{\lambda}_i^k$ can be viewed as the price for active power and reactive power, respectively. Fig. 2 illustrates the proposed IEC 61850 implementation.
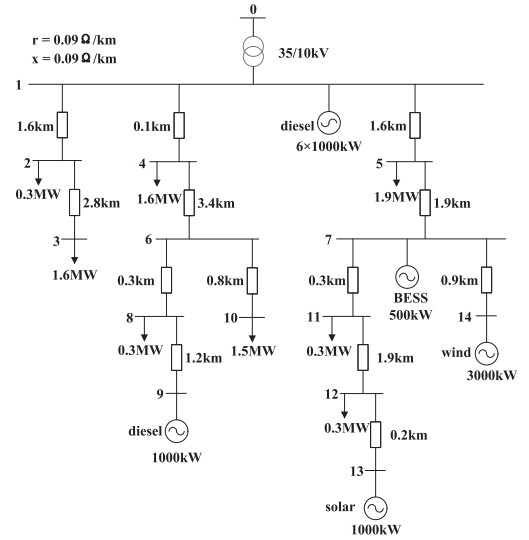
Algorithm 1 needs a few updates to support the proposed IEC 61850 implementation. In step 3, the MGCC sends the control signals by writing to the DSCH LNs of the price for active and reactive power. In step 4, after the LC solves the EMS-LC problem using the control signals read from the DSCH LNs of the prices, the new schedules are written to the corresponding DSCH LNs. In step 6, the LC sends the new schedules to the MGCC using the IEC 61850 report control block (RCB) mechanism. At convergence, the optimal schedules will be stored in the DSCH LNs and used to control the DER device.

V. PERFORMANCE EVALUATION

In this section, we demonstrate the proposed distributed EMS by applying it to a real microgrid. We first describe the microgrid system and the setup used in the simulation. We then present the simulation results in islanded and grid-connected mode followed by the discussions on the location effect, the load shedding/shifting, the ramping constraint, and the trade-offs in the objective.

A. Simulation Setup

Fig. 3 shows the configuration of a real microgrid in Guangdong Province, China. The numbers under the DERs and the loads in the figure correspond to the maximum power. We use this microgrid to demonstrate the proposed distributed EMS. In the simulation, a day starts from 12 A.M. The time interval Δt in the model is 1 h and we denote a day by $\mathcal{T} \triangleq \{0, 1, \ldots, 23\}$, where each $t \in \mathcal{T}$ denotes the hour of $[t, t+1]$.

We set the cost function of the diesel generation as $C_g(p_g(t)) \triangleq 10(p_g(t)\Delta t)^2 + 70(p_g(t)\Delta t)$. The generation ramping parameter r_g is chosen to be 0.3. The capacity of the BESS $\bar{E}_b$ is 3 MWh and $\underline{E}_b$ is chosen to be 0.1 MWh. We set $E_b(0) = 1.5$ MWh, $E_b^e = 1.0$ MWh, and $\eta_b = 0.95$. The parameters in the cost function of the battery are chosen as $\alpha_b = 1$, $\beta_b = 0.75$, and $\gamma_b = 0.5$. We choose $\alpha_l = 10^3$ and
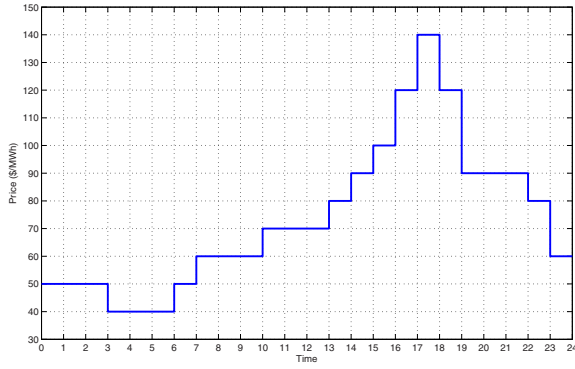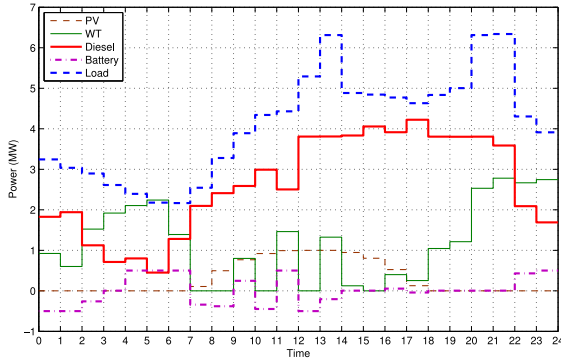
Fig. 4.   Day-ahead price from CAISO.

Fig. 6.   Output schedules in grid-connected mode.

Fig. 5.   Output schedules in islanded mode.

Fig. 7.   Net power injected to the microgrid.

$\alpha_l = 10^2$ in the cost function of the interruptible and deferrable loads, respectively. We assume that bus 5 is a deferrable load and the rest of the loads are all interruptible. For the interruptible loads, the maximum load shedding percentage is chosen randomly from the range [20%, 50%]. For the deferable load, the start time is chosen randomly from [10, 13] and the deadline is chosen randomly from [20, 23]. The minimum energy requirement $\underline{E}_l$ is chosen randomly from $[3\bar{p}_l, 5\bar{p}_l]$ and the energy upper bound is set to be $\bar{E}_l = \underline{E}_l + 2\bar{p}_l$, where $\bar{p}_l$ is the maximum power of load l. Perfect forecasting of the PV, the WT, and the loads is assumed. For the forecasting of the deferrable load, we assume that the load consumes power at the maximum rate from the start time until the consumed energy reaches the energy upper bound. We use the real day-ahead energy price from California ISO (CAISO) in the simulation as shown in Fig. 4.

B. Case Study

We apply the proposed EMS to the microgrid using the setup described above. The voltage tolerances are set to be [0.95 p.u., 1.05 p.u.]. The parameters in the algorithm are chosen as $\xi_g = 1$, $\xi_b = 1$, $\xi_l = 1$, $\xi_0 = 1$, $\xi_p = 1$, and $\gamma = 0.75$.

The day-ahead schedules produced by the proposed EMS in islanded mode is shown in Fig. 5. In islanded mode, the microgrid can utilize only the DERs to serve the loads. Since the nondispatchable renewable generations (i.e., PV and WT) in the microgrid only serve for a small proportion of the loads, diesel is the main power source. From the figure, we can see that the total diesel generation changes in the same trend as
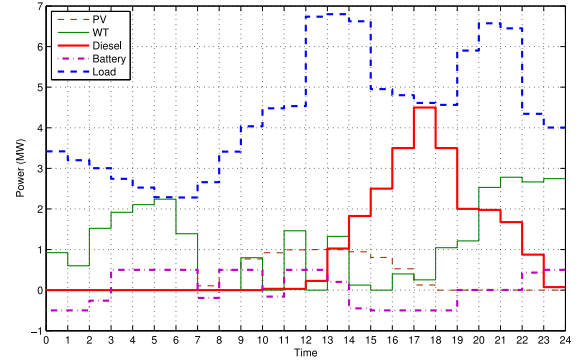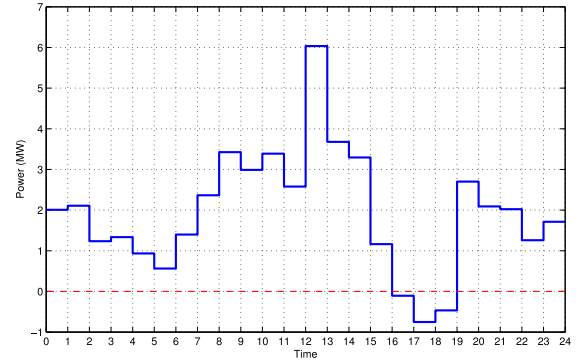
the total load. We can also observe the charging/discharging cycles of the battery from the figure. The battery is charged when the renewable generation is high and discharged when it is low, serving as the storage for the renewables in the microgrid.

Fig. 6 shows the results in grid-connected mode. Compared with Fig. 5, the total diesel generation is decreased significantly in grid-connected mode. Diesel generation is no longer the main power source in grid-connected mode as the microgrid is able to import power from the main grid. The battery in grid-connected mode is the storage for not only the renewables, but also the cheap power from the main grid. It is also charged when the energy price is low and discharged when the energy price is high, making profits for the microgrid.

The net power injected to the microgrid in grid-connected mode is shown in Fig. 7. It can be seen from the figure that the microgrid imports power when the energy price is low and exports power when the price is high ($t \in [16, 18]$). If we compare the total operational cost of the microgrid (i.e., the value of the objective function) in the two modes, we can find that grid-connected mode decreases the operational cost by ($\$6491 - \$5484)/\$6491 = 15.5\%$.

Fig. 8 shows the dynamics of EMS-MGCC and EMS-LC in grid-connected mode. We can see that our proposed distributed algorithm converges fast. For the simulations, we also verify that the solution to the centralized OPF-r problem is the same as the solution to the distributed algorithm. We further verify
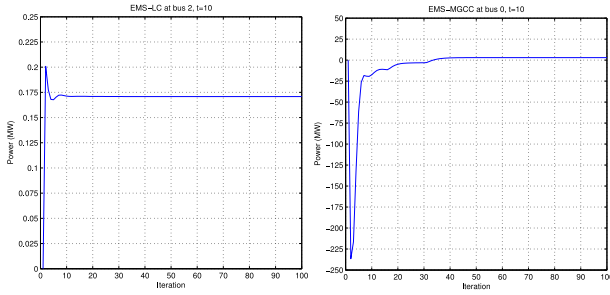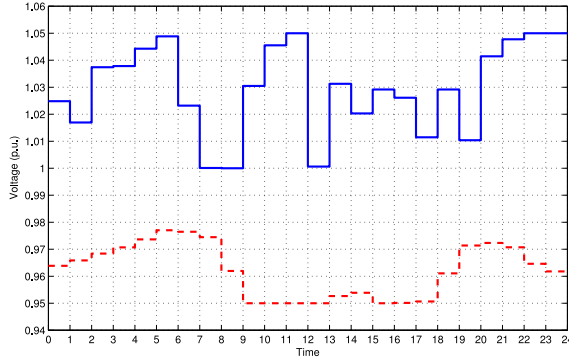
Fig. 8.   Dynamics of EMS-MGCC and EMS-LC.

Fig. 9.   Maximum and minimum bus voltage in the microgrid.

Fig. 10.   Demand reduction of the loads.

Fig. 11.   Load shifting.

that the equality in (27) is attained in the optimal solution to OPF-r, i.e., OPF-r is an exact relaxation of OPF.

C. Discussion

1) Location Effect: In order to exemplify the effect on voltage tolerances, we increase the line lengths by five times. Fig. 9 shows the maximum and the minimum bus voltage in the microgrid over time. It can be seen from the figure that the bus voltages in the microgrid are well maintained within the allowed range. The maximum voltage reaches the upper bound when the nondispatchable renewable generation is high and the minimum voltage reaches the lower bound when the load is high. This is because the generation injects power to the distribution network and hence increases the voltage, while the load consumes power and thus decreases the voltage.

In order to understand how the voltage tolerances are maintained by the proposed EMS, we look into the demand reduction of each load as shown in Fig. 10. From the figure, it can be easily seen that the demand reduction of bus 2 and 3 is significantly more than the other buses. This is because both bus 2 and 3 are far from the generation or the feeder and thus the voltage drop along the line is significant. Therefore, more demand reduction is required at bus 2 and 3 in order to maintain the bus voltage above the minimum allowed voltage. Similarly, those loads close to the nondispatchable renewable generation (bus 11 and 12) need to consume more in order to reduce the high voltage due to the generation, leading to less demand reduction. The result shows the location effect that a DSM scheme may discriminate the loads based on their locations [12].
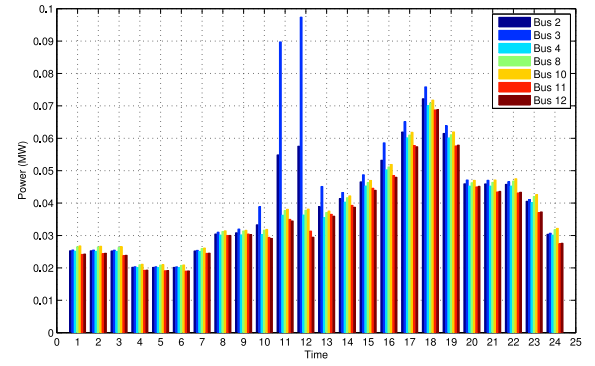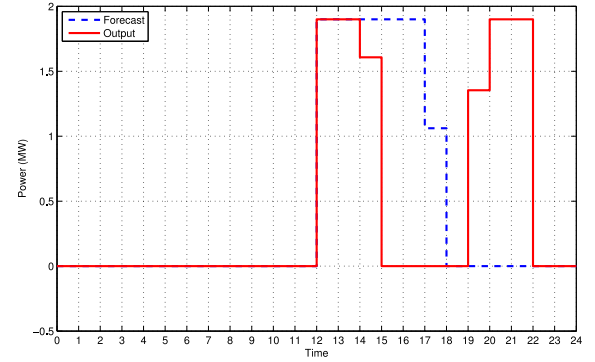
2) Load Shedding/Shifting: Fig. 10 also illustrates how the loads are shedded in grid-connected mode. As can be expected, the loads are shedded in response to the price: more loads are shedded when the price is high in order to save cost. In islanded mode, load shedding is mainly used to balance the local supply. If we compare the total amount of shedded loads in the two modes, we can find that islanded mode (8.91 WM) makes more load shedding than grid-connected mode (6.21 MW).

Fig. 11 shows the load shifting in grid-connected mode. As can be seen from the figure, the load is shifted from the time when the energy price is high ($t \in [14, 17]$) to when the price is low ($t \in [19, 21]$). The total consumed energy with load shifting is the same as without load shifting.

3) Ramping Constraint: Fig. 12 illustrates the effect of the ramping constraint on the objective. As can be seen from the figure, the total cost is nonincreasing with the ramping parameter r_g in both islanded and grid-connected mode. This is because the stricter the ramping constraint is, the less available power the diesel generation can provide. It can be also seen from the figure that the marginal cost decreases in both modes as r_g increases. In particular, the cost does not decrease much when $r_g \geq 0.3$, showing that the diesel generation supply is relatively sufficient in that region of r_g. Furthermore, the marginal cost in islanded mode decreases much faster than in grid-connected mode when r_g is small. This is easy to understand as diesel is the main power supply in islanded mode and a strict ramping constraint on it would cause more load shedding/shifting that leads to a higher cost.
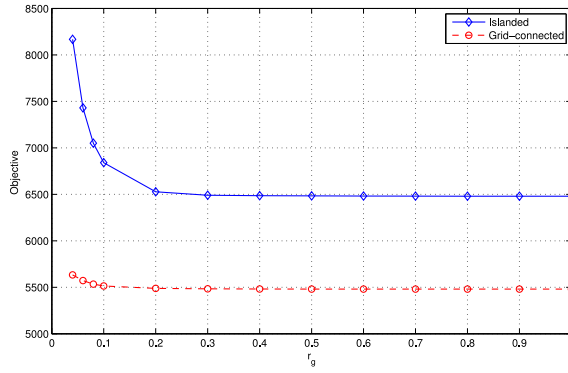
Fig. 12. Effect of r_g on the objective.

TABLE I
COST COMPARISON UNDER DIFFERENT ξ

	Diesel	Battery	Load	Purchase	Loss
Baseline	2053.14	3.20	259.37	3167.49	0.43
$\xi_g = 10$	0.00	3.19	260.21	5743.28	0.49
$\xi_b = 10^2$	2053.23	0.27	259.45	3239.15	0.43
$\xi_l = 10$	2054.93	3.20	2.60	3632.65	0.44
$\xi_0 = 10$	19408.20	3.93	12999.53	−9245.71	0.39
$\xi_p = 10^4$	2871.53	3.45	476.58	2402.79	0.34

4) Trad-Offs in the Objective: In the objective function of the optimization, there are several parameters $(\xi_g, \xi_b, \xi_l, \xi_0, \xi_p)$. Each ξ is associated with one cost minimization in the optimization. To evaluate their effects on the proposed EMS, we conduct simulations using different ξ. We choose the baseline as the set of parameters used in our previous simulation. We then change the parameter ξ one at a time and compare the individual costs as shown in Table I.

As can be seen from the table, the parameter ξ affects the trade-offs among different cost minimizations. A large ξ would decrease the corresponding cost in the optimization. The choice of ξ depends on the importance of the corresponding cost minimization in energy management. For example, if the microgrid operator is more interested in minimizing the generation cost, ξ_g can be increased and the resulting generation cost would be decreased.

VI. CONCLUSION

In this paper, we propose a distributed EMS for the optimal operation of microgrids. Compared with the existing distributed approaches, our proposed EMS considers the underlying power distribution network and the associated constraints. Specifically, we formulate microgrid energy management as an OPF problem and propose a distributed EMS where the MGCC and the LCs jointly compute an optimal schedule. We also provide an implementation of the proposed EMS based on the IEC 61850 standard. As one demonstration, we apply the proposed EMS to a real microgrid in Guangdong Province, China. The simulation results demonstrate that the proposed EMS is effective in both islanded and grid-connected mode. It is shown that the proposed distributed algorithm converges fast. A comprehensive analysis of its performance is given. Future work includes implementing the proposed EMS in a real system and analyzing its performance.

APPENDIX

Introduction to PCPM

In this paper, we develop a distributed EMS using the PCPM algorithm [23]. PCPM is a decomposition method for solving convex optimization problem. At each iteration, it computes two proximal steps in the dual variables and one proximal step in the primal variables. We give a very brief description of the PCPM algorithm below.

Consider a convex optimization problem with separable structure of the form

$$\min_{\mathbf{x} \in \mathcal{X}, \mathbf{y} \in \mathcal{Y}} f(\mathbf{x}) + g(\mathbf{y}) \tag{28}$$

$$\text{s.t.} \quad A\mathbf{x} + B\mathbf{y} = \mathbf{c}. \tag{29}$$

Let $\mathbf{z}$ be the Lagrangian variable for the constraint (29). The steps of the PCPM algorithm to solve the problem are given as follows.

1) Initially set $k \leftarrow 0$ and choose the initial $(\mathbf{x}^0, \mathbf{y}^0, \mathbf{z}^0)$ randomly.
2) For each $k \geq 0$, update a virtual variable $\hat{\mathbf{z}}^k := \mathbf{z}^k + \gamma(A\mathbf{x}^k + B\mathbf{y}^k - \mathbf{c})$ where $\gamma > 0$ is a constant step size.
3) Solve

$$\mathbf{x}^{k+1} = \arg\min_{\mathbf{x} \in \mathcal{X}} \left\{ f(\mathbf{x}) + \left(\hat{\mathbf{z}}^k\right)^T A\mathbf{x} + \frac{1}{2\gamma} \left\| \mathbf{x} - \mathbf{x}^k \right\|^2 \right\},$$

$$\mathbf{y}^{k+1} = \arg\min_{\mathbf{y} \in \mathcal{Y}} \left\{ g(\mathbf{y}) + \left(\hat{\mathbf{z}}^k\right)^T B\mathbf{y} + \frac{1}{2\gamma} \left\| \mathbf{y} - \mathbf{y}^k \right\|^2 \right\}.$$

4) Update $\mathbf{z}^{k+1} := \mathbf{z}^k + \gamma(A\mathbf{x}^{k+1} + B\mathbf{y}^{k+1} - \mathbf{c})$.
5) $k \leftarrow k + 1$, and go to step 2 until convergence.

Steps 2 and 4 can be seen as a predictor step and a corrector step to the Lagrange multiplier, respectively. It has been shown in [23] that the above algorithm will converge to a primal-dual optimal solution $(\mathbf{x}^*, \mathbf{y}^*, \mathbf{z}^*)$ for a sufficient small positive step size γ as long as strong duality holds for the convex problem (28).

REFERENCES

[1] W. Shi, X. Xie, C.-C. Chu, and R. Gadh, "A distributed optimal energy management strategy for microgrids," in *Proc. IEEE Int. Conf. Smart Grid Commun. (SmartGridComm)*, Venice, Italy, Nov. 2014, pp. 206–211.
[2] F. Katiraei, R. Iravani, N. Hatziargyriou, and A. Dimeas, "Microgrids management," *IEEE Power Energy Mag.*, vol. 6, no. 3, pp. 54–65, May 2008.
[3] S. Choi, S. Park, D.-J. Kang, S.-J. Han, and H.-M. Kim, "A microgrid energy management system for inducing optimal demand response," in *Proc. IEEE Int. Conf. Smart Grid Commun. (SmartGridComm)*, Brussels, Belgium, Oct. 2011, pp. 19–24.
[4] C. Cecati, C. Citro, and P. Siano, "Combined operations of renewable energy systems and responsive demand in a smart grid," *IEEE Trans. Sustain. Energy*, vol. 2, no. 4, pp. 468–476, Oct. 2011.

[5] S. Pourmousavi, M. Nehrir, C. Colson, and C. Wang, "Real-time energy management of a stand-alone hybrid wind-microturbine energy system using particle swarm optimization," *IEEE Trans. Sustain. Energy*, vol. 1, no. 3, pp. 193–201, Oct. 2010.

[6] P. Siano, C. Cecati, H. Yu, and J. Kolbusz, "Real time operation of smart grids via FCN networks and optimal power flow," *IEEE Trans. Ind. Informat.*, vol. 8, no. 4, pp. 944–952, Nov. 2012.

[7] A. Dimeas and N. Hatziargyriou, "Operation of a multiagent system for microgrid control," *IEEE Trans. Power Syst.*, vol. 20, no. 3, pp. 1447–1455, Aug. 2005.

[8] Z. Wang, K. Yang, and X. Wang, "Privacy-preserving energy scheduling in microgrid systems," *IEEE Trans. Smart Grid*, vol. 4, no. 4, pp. 1810–1820, Dec. 2013.

[9] A. Dominguez-Garcia and C. Hadjicostis, "Distributed algorithms for control of demand response and distributed energy resources," in *Proc. IEEE Conf. Decis. Control Eur. Control (CDC)*, Orlando, FL, USA, Dec. 2011, pp. 27–32.

[10] Y. Zhang, N. Gatsis, and G. Giannakis, "Robust energy management for microgrids with high-penetration renewables," *IEEE Trans. Sustain. Energy*, vol. 4, no. 4, pp. 944–953, Oct. 2013.

[11] E. Crisostomi, M. Liu, M. Raugi, and R. Shorten, "Plug-and-play distributed algorithms for optimized power generation in a microgrid," *IEEE Trans. Smart Grid*, vol. 5, no. 4, pp. 2145–2154, Jul. 2014.

[12] W. Shi, N. Li, X. Xie, C.-C. Chu, and R. Gadh, "Optimal residential demand response in distribution networks," *IEEE J. Sel. Areas Commun.*, vol. 32, no. 7, pp. 1441–1450, Jul. 2014.

[13] S. H. Low, "Convex relaxation of optimal power flow—Part I: Formulations and equivalence," *IEEE Trans. Control Netw. Syst.*, vol. 1, no. 1, pp. 15–27, Mar. 2014.

[14] S. H. Low, "Convex relaxation of optimal power flow—Part II: Exactness," *IEEE Trans. Control Netw. Syst.*, vol. 1, no. 2, pp. 177–189, Jun. 2014.

[15] N. Li, L. Chen, and S. H. Low, "Exact convex relaxation of OPF for radial networks using branch flow model," in *Proc. IEEE Int. Conf. Smart Grid Commun. (SmartGridComm)*, Tainan, Taiwan, Nov. 2012, pp. 7–12.

[16] L. Gan, N. Li, U. Topcu, and S. H. Low, "On the exactness of convex relaxation for optimal power flow in tree networks," in *Proc. IEEE Conf. Decis. Control Eur. Control (CDC)*, Maui, HI, USA, Dec. 2012, pp. 465–471.

[17] L. Gan, N. Li, U. Topcu, and S. H. Low, "Optimal power flow in tree networks," in *Proc. IEEE Conf. Decis. Control Eur. Control (CDC)*, Florence, Italy, Dec. 2013, pp. 2313–2318.

[18] L. Gan, N. Li, U. Topcu, and S. H. Low, "Exact convex relaxation of optimal power flow in radial networks," *IEEE Trans. Autom. Control*. [Online]. Available: http://ieeexplore.ieee.org/xpl/articleDetails.jsp?tp=&arnumber=6843918

[19] L. Gan and S. H. Low, "Convex relaxations and linear approximation for optimal power flow in multiphase radial networks," arxiv:1406.3054, 2014. [Online]. Available: http://arxiv.org/abs/1406.3054

[20] R. Huang, T. Huang, R. Gadh, and N. Li, "Solar generation prediction using the ARMA model in a laboratory-level micro-grid," in *Proc. IEEE Int. Conf. Smart Grid Commun. (SmartGridComm)*, Tainan, Taiwan, Nov. 2012, pp. 528–533.

[21] G. Sideratos and N. Hatziargyriou, "An advanced statistical method for wind power forecasting," *IEEE Trans. Power Syst.*, vol. 22, no. 1, pp. 258–265, Feb. 2007.

[22] N. Li, L. Chen, and S. H. Low, "Optimal demand response based on utility maximization in power networks," in *Proc. IEEE Power Energy Soc. Gen. Meeting (PES GM)*, San Diego, CA, USA, Jul. 2011, pp. 1–8.

[23] G. Chen and M. Teboulle, "A proximal-based decomposition method for convex minimization problems," *Math. Program.*, vol. 64, no. 1, pp. 81–101, Mar. 1994.

[24] Q. Peng and S. H. Low, "Distributed algorithm for optimal power flow on a radial network," 2014. [Online]. Available: http://arxiv.org/abs/1404.0700

[25] R. Huang, E.-K. Lee, C.-C. Chu, and R. Gadh, "Integration of IEC 61850 into a distributed energy resources system in a smart green building," in *Proc. IEEE Power Energy Soc. Gen. Meeting (PES GM)*, National Harbor, MD, USA, Jul. 2014, pp. 1–5.

[26] *Communication Networks and Systems for Power Utility Automation—Part 7-420: Basic Communication Structure—Distributed Energy Resources Logical Nodes,* IEC Standard 61850-7-420, 2009.

Wenbo Shi (S'08) received the B.S. degree from Xi'an Jiaotong University, Xi'an, China, and the M.A.Sc. degree from the University of British Columbia, Vancouver, BC, Canada, in 2009 and 2011, respectively, both in electrical engineering. He is currently pursuing the Ph.D. degree from the Smart Grid Energy Research Center, University of California, Los Angeles, CA, USA.

His current research interests include demand response, microgrids, and energy management systems.

Xiaorong Xie (M'02) received the B.Sc. degree from Shanghai Jiao Tong University, Shanghai, China, and the Ph.D. degree from Tsinghua University, Beijing, China, in 1996 and 2001, respectively.

He is an Associate Professor with the Department of Electrical Engineering, Tsinghua University. His current research interests include analysis and control of microgrids, and flexible ac transmission systems.

Chi-Cheng Chu received the B.S. degree from National Taiwan University, Taipei, Taiwan, and the Ph.D. degree from the University of Wisconsin–Madison, Madison, WI, USA, in 1990 and 2001, respectively.

He is currently a Project Lead with the Smart Grid Energy Research Center, University of California, Los Angeles, CA, USA. He is a seasoned Research Manager who supervised and steered multiple industry and academia research projects in the field of smart grid, radio frequency identification technologies, mobile communication, media entertainment, 3-D/2-D visualization of scientific data, and computer aided design.

Rajit Gadh received the Bachelor's degree from the Indian Institute of Technology, Kanpur, India; the Master's degree from Cornell University, Ithaca, NY, USA; and the Ph.D. degree from Carnegie Mellon University, Pittsburgh, PA, USA, in 1984, 1986 and 1991, respectively.

He is a Professor with the Henry Samueli School of Engineering and Applied Science, University of California, Los Angeles (UCLA), CA, USA, and the Founding Director of the UCLA Smart Grid Energy Research Center, Los Angeles. His current research interests include smart grid architectures, smart wireless communications, sense and control for demand response, microgrids and electric vehicle integration into the grid, and mobile multimedia.